Current Research in Toxicology 5 (2023) 100134

Contents lists available at ScienceDirect

Current Research in Toxicology

journal homepage: www.journals.elsevier.com/current-research-in-toxicology

Potential roles of 4HNE-adducted protein in serum extracellular vesicles as an early indicator of oxidative response against doxorubicin-induced cardiomyopathy in rats

Chontida Yarana [a], Chayodom Maneechote [d,e,f], Thawatchai Khuanjing [d,e,f], Benjamin Ongnok [d,e,f], Nanthip Prathumsap [d,e,f], Sirasa Thanasrisuk [b], Kovit Pattanapanyasat [c], Siriporn C. Chattipakorn [e,f,g], Nipon Chattipakorn [d,e,f,*]

[a] Center for Research Innovation and Biomedical Informatics, Faculty of Medical Technology, Mahidol University, 999 Phuttamonthon 4 Road, Salaya, Nakhon Pathom 73170, Thailand
[b] Faculty of Medical Technology, Mahidol University, 999 Phuttamonthon 4 Road, Salaya, Nakhon Pathom 73170, Thailand
[c] Center of Excellence for Microparticle and Exosome in Diseases, Department of Research and Development, Faculty of Medicine Siriraj Hospital, Mahidol University, Bangkok 10700, Thailand
[d] Cardiac Electrophysiology Research and Training Center, Faculty of Medicine, Chiang Mai University, Chiang Mai 50200, Thailand
[e] Cardiac Electrophysiology Unit, Department of Physiology, Faculty of Medicine, Chiang Mai University, Chiang Mai 50200, Thailand
[f] Center of Excellence in Cardiac Electrophysiology Research, Chiang Mai University, Chiang Mai 50200, Thailand
[g] Department of Oral Biology and Diagnostic Sciences, Faculty of Dentistry, Chiang Mai University, Chiang Mai 50200, Thailand

ARTICLE INFO

Keywords:
Doxorubicin
Cardiomyopathy
4-hydroxynonenal
Extracellular vesicles
Biomarkers
Oxidative response

ABSTRACT

Late-onset cardiomyopathy is becoming more common among cancer survivors, particularly those who received doxorubicin (DOXO) treatment. However, few clinically available cardiac biomarkers can predict an unfavorable cardiac outcome before cell death. Extracellular vesicles (EVs) are emerging as biomarkers for cardiovascular diseases and others. This study aimed to measure dynamic 4-hydroxynonenal (4HNE)-adducted protein levels in rats treated chronically with DOXO and examine their link with oxidative stress, antioxidant gene expression in cardiac tissues, and cardiac function. Twenty-two male Wistar rats were randomly assigned to receive intraperitoneal injection of normal saline (n = 8) or DOXO (3 mg/kg, 6 doses, n = 14). Before and after therapy, serum EVs and N-terminal pro-B-type natriuretic peptide (NT-proBNP) levels were determined. Tunable resistive pulse sensing was used to measure EV size and concentration. ELISA was used to assess 4HNE-adducted protein in EVs and cardiac tissues. Differential-display reverse transcription-PCR was used to quantitate cardiac *Cat* and *Gpx1* gene expression. Potential correlations between 4HNE-adducted protein levels in EVs, cardiac oxidative stress, antioxidant gene expression, and cardiac function were determined. DOXO-treated rats showed more serum EV 4HNE-adducted protein than NSS-treated rats at day 9 and later endpoints, whereas NT-proBNP levels were not different between groups. Moreover, on day 9, surviving rats' EVs had higher levels of 4HNE-adducted protein, and these correlated positively with concentrations of heart tissue 4HNE adduction and copy numbers of *Cat* and *Gpx1*, while at endpoint correlated negatively with cardiac functions. Therefore, 4HNE-adducted protein in serum EVs could be an early, minimally invasive biomarker of the oxidative response and cardiac function in DOXO-induced cardiomyopathy.

Abbreviations: DOXO, Doxorubicin; NSS, Normal saline solution; NT-proBNP, N-terminal pro B-type natriuretic peptide; EVs, Extracellular vesicles; 4HNE, 4-hydroxynonenal; NSS_EVs, EVs collected from NSS-treated rat serum; DOXO_EVs, EVs collected from DOXO-treated rat serum; NSS_Heart, Left venticles from NSS-treated rats; DOXO_Heart, Left venticles from DOXO-treated rats; NSS_Brain, Forebrains from NSS-treated rats; DOXO_Brain, Forebrains from DOXO-treated rats; TRPS, Tunable resistive pulse sensing; %LVEF, Left ventricular ejection fraction; %LVFS, left ventricular fractional shortening; *Cat*, Catalase gene; *Gpx1*, Glutathione peroxidase-1 gene; BBB, Blood-brain barrier.

* Corresponding author.
E-mail addresses: chontida.yar@mahidol.edu (C. Yarana), chayodom.man@gmail.com (C. Maneechote), wat23005@hotmail.com (T. Khuanjing), benjamin.aongnok@gmail.com (B. Ongnok), nanthip.pra28@gmail.com (N. Prathumsap), sirasa.tha@student.mahidol.edu (S. Thanasrisuk), kovit.pat@mahidol.ac.th (K. Pattanapanyasat), scchattipakorn@gmail.com (S.C. Chattipakorn), nipon.chat@cmu.ac.th (N. Chattipakorn).

https://doi.org/10.1016/j.crtox.2023.100134
Received 28 June 2023; Received in revised form 18 October 2023; Accepted 31 October 2023
Available online 3 November 2023

Introduction

A significant increase in the number of long-term cancer survivors is a primary concern for late-onset side effects of cancer treatment, especially chemotherapies, which can induce fatal cardiomyopathy (Shakir and Rasul, 2009; Watson et al., 2022). The risk of death among chemotherapy-treated patients increases over time after treatment (Sturgeon et al., 2019). Doxorubicin (DOXO) is frequently used for the therapy of a wide range of solid tumors and hematologic malignancies. However, it also generates excessive oxidative stress and is a well-known cause of life-threatening cardiomyopathy (Songbo et al., 2019). The oxidative stress in cardiac muscle is stimulated by the production of pro-oxidants and inhibition of antioxidant enzymes. This results in the accumulation of products of this oxidative damage and may ultimately lead to cell death through multiple pathways, including ferroptosis, necroptosis and apoptosis (Sangweni et al., 2022). To date, the clinically available biomarkers of cardiac injury are cardiac troponin and N-terminal pro B-type natriuretic peptide (NT-proBNP) (Ananthan & Lyon, 2020). The cardiac-specific troponins I and T released after irreversible cardiac injury are the most sensitive and specific biomarkers of acute myocardial infarction (Hammarsten et al., 2022; Ibanez et al., 2018) as well as injury from other causes including chemotherapy (Newby et al., 2011; Sorodoc et al., 2022; Tian et al., 2014). NT-proBNP is widely used as a significant indicator of clinical heart failure (Chow et al., 2017; Maalouf and Bailey, 2016; Troughton et al., 2014), and is also a potential biomarker for asymptomatic cardiomyopathy in DOXO-treated patients (Kittiwarawut et al., 2013; Sherief et al., 2012; Sulaiman et al., 2021; Zidan et al., 2015). Unfortunately, using cardiac troponin or NT-proBNP as a guide for initiating preventive intervention for DOXO-induced cardiomyopathy may be too late, as they are released after cardiac cell death has occurred, which is an irreversible process. For prompt preventive intervention against this fatal condition, earlier biomarkers are needed.

Extracellular vesicles (EVs) are nano-sized membrane-bound particles that are secreted from numerous cellular locations and processes and are found in blood and other body fluids (Campanella et al., 2019). EVs are released by cells to deliver signaling molecules, respond to stress stimuli, and eliminate waste or unneeded material. EVs exhibit significant potential as innovative biomarkers in liquid biopsy due to their abundant presence in body fluids and involvement in several physiological and pathological mechanisms. EVs possess a wide range of information that mirrors the condition of living cells. Their ability to remain stable in circulation and body fluids renders them a promising reservoir of biomarkers for various diseases, especially cancer. Consequently, EVs hold potential for applications in cancer diagnosis, treatment monitoring, prognosis and adverse effect prediction (Cheng et al., 2022; Yu et al., 2022; Zhou et al., 2020).

Excessive amounts of reactive oxygen species (ROS) and reactive nitrogen species (RNS) can disrupt cell signaling, and in turn change the volume and composition of EVs (Chiaradia et al., 2021). EVs transport oxidized lipids, proteins, and cargo molecules that can modulate the redox status of their target cells (Benedikter et al., 2018; Yarana & St Clair, 2017). The polyunsaturated fatty acids of biological membranes are susceptible to attack by ROS, the process known as lipid peroxidation. 4-hydroxynonenal (4HNE) is a highly reactive aldehyde byproduct of this lipid peroxidation that can covalently bind to proteins, causing their inactivation and cytotoxicity. Large bodies of evidence have shown that 4HNE inhibits cardiac contractile function, increases ROS generation, changes cell signaling pathways and is linked to a variety of cardiovascular disorders, including atherosclerosis (Chapple et al., 2013; Leonarduzzi et al., 2005), myocardial ischemia–reperfusion injury (Gao et al., 2023; Zhang et al., 2010), heart failure (Asselin et al., 2007; Hwang et al., 2020), and cardiomyopathy (Mali & Palaniyandi, 2014; Singh et al., 2015). 4HNE plays an important role in DOXO-induced cardiotoxicity. Even non-toxic doses of DOXO could result in the accumulation of 4HNE-adducted proteins by cardiomyocytes, which show a wide range of individuality (Negre-Salvayre et al., 2010). Increased levels of 4HNE upon DOXO treatment inactivate NADH oxidoreductase activity of the mitochondrial apoptosis-inducing factor (AIFm2) causing 4HNE adduction and translocation of AIFm2 from mitochondria leading to apoptosis in heart tissue of mice and humans (Miriyala et al., 2016). Multiple studies have demonstrated that DOXO treatment increased the formation of 4HNE within cardiac tissue (Chaiswing et al., 2005; Jungsuwadee et al., 2006; Jungsuwadee et al., 2009). The accumulation of 4HNE in cardiac tissue may be interpreted as a result of the oxidative stress, which induce cardiac dysfunction and, consequently, cardiomyopathy.

A previous study in mice revealed that after a single high dose of DOXO, serum EVs contain increased levels of 4HNE-adducted protein and of a cardiac tissue-specific protein (brain-type glycogen phosphorylase) which can be detected prior to the rise in serum of cardiac troponin-I (Yarana et al., 2018). However, the dynamic change of 4HNE-adducted protein levels in EVs during chronic DOXO treatment in comparison with cardiac injury biomarkers have never been reported. Using chronic DOXO-treated rodents as a model, we investigated the time course of changes in 4HNE-adducted protein levels in serum EVs and found associations with cardiac tissue injury, cardiac tissue oxidative stress, and survival outcome.

This study will strengthen the clinical significance of 4HNE-adducted protein levels in serum EVs in predicting the development of adverse effects of DOXO, especially cardiomyopathy, hopefully leading to the future development of a new diagnostic to aid physicians in deciding on intervention to prevent this adverse outcome.

Materials and methods

Ethical approval

Ethical approval for this study was obtained from the Laboratory Animal Center, Chiang Mai University, Chiang Mai, Thailand (approval no. 2562/RT-0008). Experiments on animals were performed in accordance with the Guide for the Care and Use of Laboratory Animals.

Animal treatment and serum collection

Male Wistar rats (n = 22) weighing 300 – 350 g were obtained from M−CLEA Nomura Siam, Thailand. The animals were transported to and kept at Chiang Mai University's Laboratory Animal Center. In a temperature-controlled setting with a 12:12 h light–dark cycle, two animals were kept in each cage, which is appropriate number related to cage size (51 x 57 x 38 cm).

All rats spent at least a week getting used to the lab environment prior to start the experiment. One week prior to treatment, 500 μL of blood was collected from the tail vein of each rat to establish baseline parameters. For this procedure and subsequent blood collections, rats were anesthetized by inhaling 3 % isoflurane; and placed in a supine position. The tail area was cleaned with an antiseptic solution and venous blood was collected. The rats were then randomly assigned to groups receiving either DOXO (n = 14) or normal saline (NSS) (n = 8). Rats in the DOXO-treated group received intraperitoneal injections of doxorubicin (ADRIM, Homburg, Germany) at a dose of 3 mg/kg on days 0, 4, 8, 15, 22, and 29, followed by a 1-month "recovery" period. The total cumulative dose was 18 mg/kg.

We chose the dose of 3 mg/kg per dose, a total of 18 mg/kg, and a one-month recovery period after the last treatment based on previous research showing that at this time point, rats treated with DOXO based on this protocol had impaired cardiac function (Arinno et al., 2021; Chunchai et al., 2022; Khuanjing et al., 2021; Maneechote et al., 2022; Yarana et al., 2022). This impairment of cardiac function is a crucial aspect to be investigated in our study.

Rats in the NSS group received injections of sterile normal saline in the same volume as those in DOXO group under the same treatment

schedule. At day 1, day 9, and day 30 after the first dose of treatment, blood samples (500 μL each) were collected via tail vein. At the endpoint on day 60, all animals were euthanized and as much blood as feasible was collected from the inferior vena cava prior to cardiac tissue collection (Fig. 1A). Blood was held at ambient temperature for at least 30 min to enable it to clot. Sera were separated and stored at −80 °C until use.

Cardiac function measurements

Using echocardiography, the cardiac functions were evaluated. During echocardiography, the rats were sedated with 2 % isoflurane and 2 L/min of oxygen flow. Using a Vivid*i (GE Healthcare, UK), echocardiographic parameters were obtained. The echocardiography probe was gently pressed against the thorax, and images were acquired along the parasternal short axis of the heart. At the level of the papillary muscles, M−mode echocardiography was conducted. The percentage of fractional shortening and ejection fraction of the left ventricle were then determined (Maneechote et al., 2019). All echocardiographic parameters were measured at the endpoint before animal euthanasia.

4HNE-adducted protein level measurement in serum EVs, sera, heart and brain tissues

Concentration of serum EVs collected from NSS-treated (NSS_EVs) and DOXO-treated rats (DOXO_EVs) at different time points was determined by bicinchoninic acid assay (BCA) (ThermoFisher Scientific, MA, USA). The concentrations were adjusted to be equal in every EV sample. One milligram of NSS_EVs or DOXO_EVs was used to measure 4HNE-adducted protein levels using OxiSelect^{TM} HNE adduct competitive ELISA kits (Cell Biolabs, CA, USA) following the protocol provided by the company. The levels of 4HNE were represented as μg of 4HNE adducted proteins per 1 mg of total protein.

Fifty microliters of sera derived from NSS-treated (NSS_Serum) or DOXO-treated rats (DOXO_Serum) at different time points were used to measure 4HNE-adducted protein levels using OxiSelect^{TM} HNE adduct competitive ELISA kits (Cell Biolabs, CA, USA) following the protocol provided by the company. The levels of 4HNE adducted protein were represented as μg/ml.

Left venticles from NSS-treated (NSS_Heart) and DOXO-treated (DOXO_Heart) rats were lysed using 1x protease inhibitor cocktails (SigmaAldrich, MO, USA) in lysis buffer containing 20 mM Tris HCl, 1 mM Na_3VO_4, 5 mM NaF. Forebrain from NSS-treated (NSS_Brain) and DOXO-treated (DOXO_Brain) rats were lysed using 1x protease inhibitor cocktails (SigmaAldrich, MO, USA) in lysis buffer containing 100 mM NaCl, 25 mM EDTA, 10 mM Tris, 1 % v/v Triton X-100, 1 % v/v NP-40.

The concentrations of heart tissue in NSS_Heart and DOXO_Heart were determined by BCA assay (ThermoFisher Scientific, MA, USA). These concentrations were then adjusted to be equal in all samples. Four hundred mg of NSS_Heart or DOXO_Heart tissue lysates were used to measure 4HNE-adducted protein levels using the OxiSelect^{TM} HNE adduct competitive ELISA kits (Cell Biolabs) following manufacturer's protocol.

Differential-display reverse transcription-PCR (ddRT-PCR)

Total RNA was extracted with the Monarch® Total RNA Miniprep Kit (New England Biolabs, Ipswich, MA, USA), following the manufacturer's instructions. Immediately following collection of hearts and brains, tissues were placed in an RNA*later* solution (Thermo Fisher Scientific, Waltham, MA, USA) and kept at −20 °C until used. Fifty milligrams of tissue were submerged and mechanically homogenized in 1 x DNA/RNA Protection Reagent. The homogenates were then treated with Proteinase K, followed by a 5-minute incubation at 55 °C. After centrifuging the homogenates at 16,000 x g for two minutes, supernatants were transferred to fresh containers. They were then mixed with RNA Lysis Buffer and transferred to a gDNA removal column. After 30 s of centrifugation at 16,000 x g, the flow-through was combined with an equal volume of

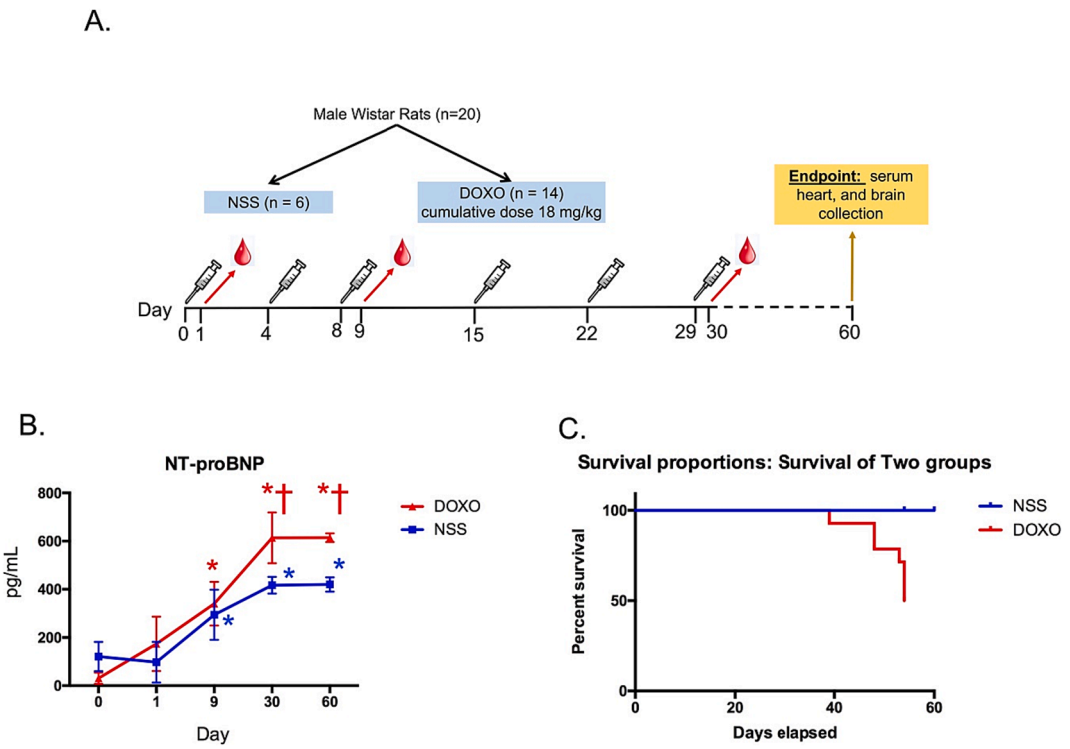

Fig. 1. Protocol of the animal treatment (A). dynamic changes of NT-proBNP levels (B). and survival curves of rats in NSS and DOXO groups (C). Syringes pictured in A represent time points of intraperitoneal injections of NSS or DOXO 3 mg/kg. Droplets of blood represent time points of blood collection. * $p < 0.05$ vs day 0 (baseline), † $p < 0.05$ vs NSS group at the same time point.

100 % ethanol and transferred to an RNA purification column. Following centrifugation and washing, 50 μL nuclease-free water was added to the center of column matrix to elute RNA. One μg of total RNA was reverse transcribed using an iScript cDNA synthesis kit (Bio-Rad, Hercules, CA, USA). Complementary DNA concentrations were determined using NanoDropTM 2000/2000c Spectrophotometer (ThermoFisher Scientific, Waltham, MA, USA). Catalase (*Cat*), glutathione peroxidase-1 (*Gpx1*), and beta-actin (*Actb*) gene copy numbers were measured in each sample using QIAcuity® EG PCR kit (Qiagen, Hilden, Germany) operated by QIAGEN's QIAcuity instrument for digital PCR (Qiagen, Hilden, Germany). The primers used in PCR reactions are listed in Table 1. The QIAcuity performs entirely automated plate priming, partition sealing, thermocycling, and image analysis. The QIAcuityTM Nanoplate 8.5 K 96-well was utilized. Each well contained 4 μL of 3x EvaGreen PCR master mix (Qiagen), 0.4μM of each forward and reverse primer, and a fixed concentration of cDNA template 0.5 μL (50 ng). The thermal cycling program consisted of 2 min at 95 °C, 40 cycles of 15 sec at 95 °C, and 30 sec at 60 °C. By dividing the number of copies of the *Actb* gene per μL of sample volume, we normalized the concentration of *Cat* and *Gpx1* genes across all samples.

EV isolation

Serum was centrifuged at 3000 x g for 15 min to remove cell debris. EVs were extracted using ExoQuick precipitation commercial reagent (System Biosciences, USA). Briefly, 50.4 μL of ExoQuick solution and 200 μL of serum were combined. The mixture was incubated at 4 °C for 30 min before being centrifuged at 1500 x g for 30 min to obtain the EV pellets. Aspiration of the supernatant was performed. The remaining ExoQuick solution was eliminated via centrifugation at 1500 x g for 5 min followed by removal of the supernatant without disturbing the pellets. Finally, the EV pellets were resuspended in phosphate buffer saline (PBS) and stored at −80 °C until used.

NT-proBNP level measurement

NT-proBNP, a biomarker of cardiac damage that has been utilized in the clinic to predict DOXO-induced cardiomyopathy, was measured in rat sera collected one week before start of DOXO or NSS therapy, and at days 1, 9, 30 and 60 following the first injections. NT-proBNP levels were determined using an ELISA kit from Elabscience (TX, USA).

EV markers detection by Western blot

The quantity of EV protein was determined using BCA assay (ThermoFisher Scientific, MA, USA). Equal quantities of this protein from the NSS and DOXO-treated groups were put onto a 10 % SDS polyacrylamide gel and electrophoresis was performed at 60 V for 30 min., followed by 100 V for 1 h. The proteins were then transferred onto PVDF membranes and blocked with 5 % non-fat dry milk in TBST for 1 h. Anti-flotillin-1 (1:1000) from Cell Signaling Technology (MA, USA), anti-Hsp70 (1:1000), and anti-CD81 antibodies (1:1000) from System Biosciences (CA, USA) were used as primary antibodies to identify EV markers. Anti-beta actin antibody (1:5000) from Cell Signaling Technology (MA, USA) was used as a primary antibody to detect a housekeeping protein in EVs. Secondary antibodies that were HRP-conjugated (System Biosciences, CA, USA) were added to the membranes after they had been washed. Protein bands were seen using the ChemiDoc MP imaging apparatus (Bio-Rad, Munich, Germany) with clarity western ECL substrate (Bio-Rad, CA, USA).

EV size and number measurement

The tunable resistive pulse sensing (TRPS) technique was performed to measure size and concentration of EVs using the Exoid (Izon Science, New Zealand). Briefly, the nanopore (NP100) membrane, which is suitable for analyzing nanoparticles with sizes between 50 and 330 nm (according to the manufacturer) was inserted into the lower fluid cell. The upper fluid cell was then put together. After soaking the nanopore with wetting solution for 5 min to allows the baseline current to stabilize, the nanopore was covered with coating solution for 10 min to prevent non-specific binding of biological nanoparticle to the nanopore membrane. Next, carboxylated polystyrene beads (Izon Science, New Zealand), designated as CPC100 with an average size of 100 nm and a stock concentration at 1.4 x 10^{13} particles/mL were used as calibration particles. CPC100 was diluted 1:1000 with measurement electrolyte (ME) buffer and used as a reference for calculation of the concentration of EV samples. Throughout the experiment, an appropriate stretch (47 mm) and voltage (700 V) were applied so that the blockades of CPC100 or EV samples in ME buffer were at least 0.5 nA above the baseline noise. The Exoid was operated as described previously (Billinge et al., 2014; Nizamudeen et al., 2018; Vogel et al., 2016). Briefly, the lower fluid cell was filled with 75 μL of ME buffer, ensuring there were no air bubbles, and the upper fluid cell was filled with 35 μL of EV sample. Sample were removed from the upper fluid cell after each measurement and replaced with ME buffer for nanopore cleaning before the next measurement. The concentration and size of calibration particles and EVs were determined at three different pressures (800, 1000, and 1400 Pa) in order to eliminate the impact of pore and particle zeta potentials on the detected concentrations.

Statistical analysis

The results were presented as mean ± standard deviation (SD). Unpaired *t* tests were used to compare the difference between NSS and DOXO groups. Two-way analysis of variance (ANOVA) was used to compare the changes in each parameter over time following treatment with NSS or DOXO. Tukey's multiple comparisons test was used to verify group differences following ANOVA. For data analysis and graphing, Excel and GraphPad Prism, version 6.0c, were used. Correlation between the levels of 4HNE-adducted protein in serum EVs or seum 4HNE-adducted protein and the levels of 4HNE adduction in heart tissues, *Cat* gene expression, *Gpx1* gene expression, %LVEF, and %LVFS was evaluated using the Pearson correlation coefficient with SPSS® Statistics version 26. A p value less than 0.05 was regarded as significant.

Results

Cardiac injury and mortality in rats treated chronically with DOXO

To simulate the clinical setting of DOXO-induced cardiotoxicity, rats received 3 mg/kg of DOXO on a periodic basis for 30 days, reaching a cumulative dose of 18 mg/kg (Fig. 1**A**). Using this protocol, we previously reported that all rats developed cardiomyopathy, as evidenced by a decrease in cardiac functions, the development of cardiac sympathovagal imbalance, and an increase in pro-apoptotic proteins in the

Table 1
List of primer sequences used in real-time RTPCR.

Gene Name	Forward Primer	Reverse Primer
Gpx1	5′- AGTTCGGACATCAGGAGAATGGCA-3′	5′- TCACCATTCACCTCGCACTTCTCA-3′
Cat	5′- GCACTACAGGCTCCGAGATGAAC-3′	5′- TTGTCGTTGCTTGGTTCTCCTTGT-3′
Actb	5′- CACTGGCATTGTGATGGACT-3′	5′- CTCTCAGCTGTGGTGGTGAA-3′

left ventricles (Yarana et al., 2022). In this study, serum NT-proBNP in the NSS group significantly increased over time beginning at day 9 post treatment. In the DOXO group, serum NT-proBNP also increased after the treatment beginning at day 9 and levels were significantly higher than that those of the NSS group at days 30 and 60 post treatment (Fig. 1**B**).

During the four weeks after the last administration of DOXO or NSS and prior to euthanize, the general health of the rats was monitored. We discovered that many of DOXO-treated rats developed severe dehydration, enlarged abdomens and ascites. Of the 14 animals in the DOXO-treated group, seven died before the endpoint. One rat died within the first two weeks, two within three weeks, and four within four weeks of their last DOXO injections. The survival curves comparing the NSS and DOXO groups are shown in Fig. 1**C**.

4HNE-adducted protein levels in heart and brain tissues

The levels of 4HNE-adducted proteins and antioxidant gene expression, including *Cat* and *Gpx1*, were used to assess oxidative stress and oxidative defense in heart and brain tissues. The DOXO-treated group's representative data (n = 7) was derived from rats that survived to the endpoint (day 60). The results show that 4HNE-adducted protein levels in heart tissues of DOXO-treated rats (DOXO_Heart) were significantly higher than those of NSS-treated rats (NSS_Heart) as shown in Fig. 2**A**. In addition, DOXO_Heart contained significantly more copies of *Gpx1* genes (Fig. 2**C**) and slightly more *Cat* genes than did NSS_Heart (Fig. 2**B**). These findings indicated that excessive oxidative stress occurred in the cardiac tissues of DOXO-treated rats, and that the surviving rats had a marked defense response against oxidative stress as evidenced by the increases in antioxidant enzymes.

Unlike cardiac tissues, there was no sign of oxidative stress in the brain tissues of the DOXO group since the levels of 4HNE-adducted protein (Fig. 2**D**), *Cat* gene expression (Fig. 2**E**), and *Gpx1* gene expression (Fig. 2**F**) were similar to those of the NSS group.

Characterization of serum EVs derived from DOXO-treated rat

The presence of EV markers and size distribution of serum EVs collected at baseline were validated using Western blotting and TRPS, respectively, to confirm that the EV isolation procedure was effective. EVs from sera of both NSS and DOXO groups contained EV markers, including flotillin-1 (a protein involved in membrane trafficking), heat shock protein 70 (Hsp70; a protein involved in vesicular export), and cluster of differentiation 81 (CD81; a tetraspanin protein), as shown in Fig. 3**A**. The size distribution revealed that most EVs were under 200 nm with a peak concentration near 90 nm (Fig. 3**B**).

The mode of EV sizes in each sample evaluated by TRPS were analyzed and presented as average size ± SD (Fig. 3**C**). At baseline, the average size of the EVs from the NSS and DOXO groups was similar (69.33 ± 5.39 vs 65.80 ± 5.22 nm). As we monitored EV size over time following treatment, we observed that the average mode of EV size of DOXO group tended to be greater at endpoint than at base line (80.17 ± 9.36 vs 65.80 ± 5.22 nm). Interestingly, the concentration of EVs in the NSS group increased substantially at day 30 after treatment initiation, but returned to baseline at the endpoint, whereas the concentration of EVs in the DOXO group increased trendily but not significantly at day 30 and at endpoint (Fig. 3**D**).

4HNE adducted protein levels in EVs as a predictor of survival outcome in DOXO-treated rats

Monitoring the levels of 4HNE-adducted protein in serum EVs over

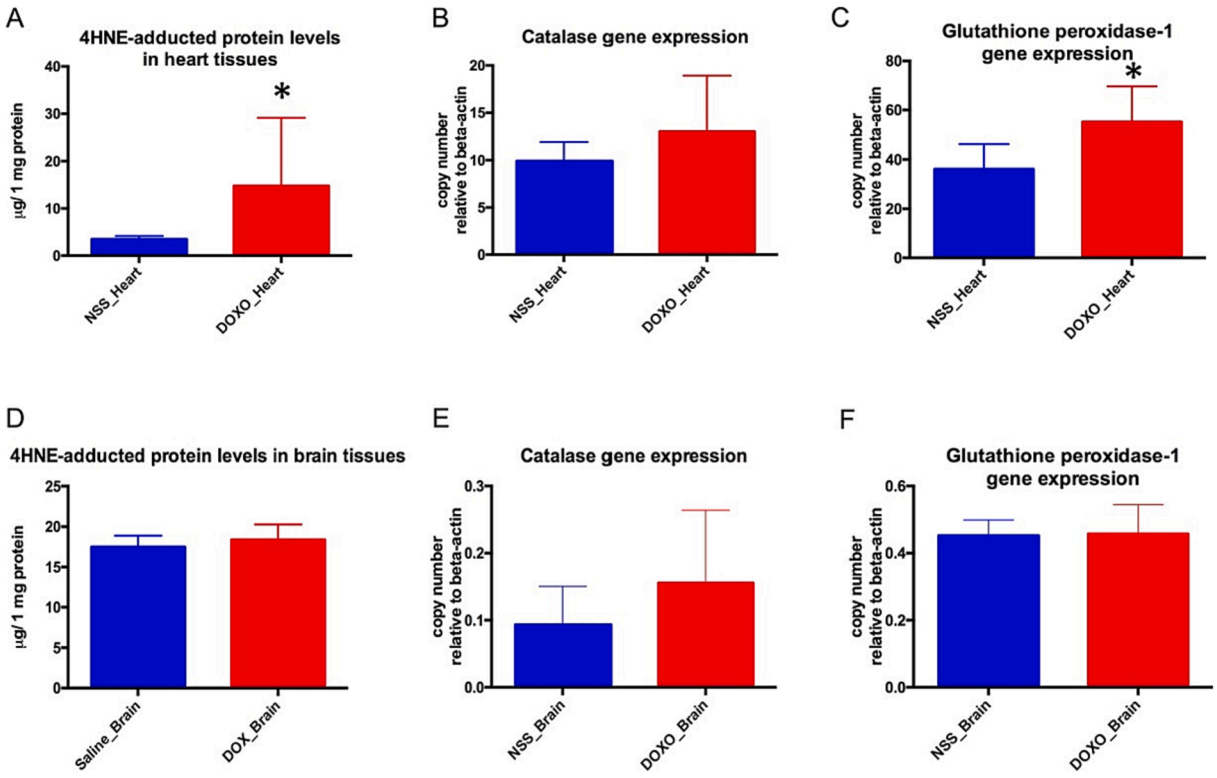

Fig. 2. Levels of 4HNE-adducted protein (μg/ 1 mg protein) in heart tissue of NSS-treated rats (NSS_Heart) and DOXO-treated rats (DOXO_Heart) (A). Levels of 4HNE-adducted protein in brain tissues of NSS-treated rats (NSS_Brain) and DOXO-treated rats (DOXO_Brain) (D). Copy number of catalase gene expression relative to beta-actin gene expression in heart tissues (B). Copy number of catalase gene expression relative to beta-actin gene expression in brain tissues (E). Copy number of glutathione peroxidase-1 gene expression relative to beta-actin gene expression in heart tissues (C). Copy number of glutathione peroxidase-1 gene expression relative to beta-actin gene expression in brain tissues (F). * $p < 0.05$ vs NSS_Heart.

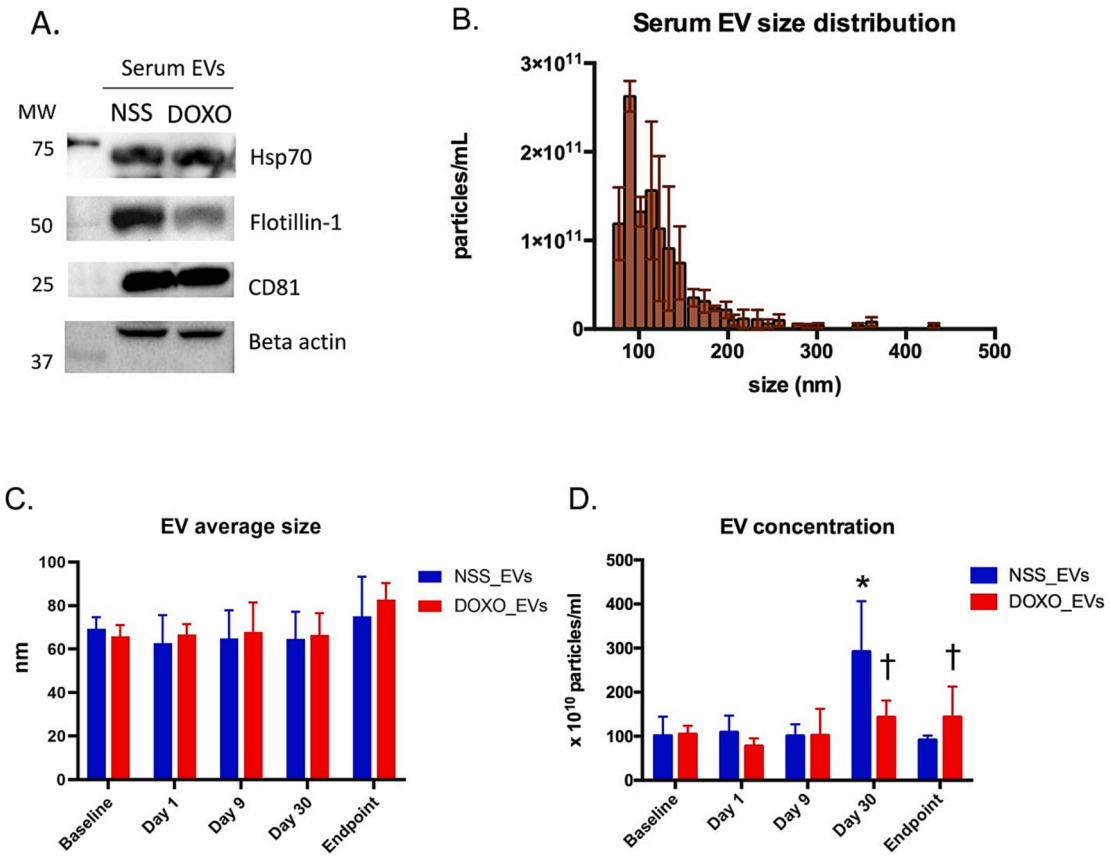

Fig. 3. Western blot of EV markers including Hsp70, flotillin-1 and CD81, as well as beta actin in serum EVs of rats treated with NSS or DOXO (A). A representative size distribution bar graph of EVs isolated from serum of rats at baseline. Each bar represents the concentration of particles per milliliter in each size range. The error bars represent the standard deviation (SD) for each concentration (B). Bar graph representing mean size of serum EVs at five time points comparing EVs from NSS-treated (NSS_EVs) and EVs from DOXO-treated (DOXO_EVs) rats (C). Bar graph representing concentrations (x 10^{10} particles/ml of serum EVs) at each time point comparing between NSS_EVs and DOXO_EVs) (D). * $p < 0.05$ vs baseline, † $p < 0.05$ vs NSS_EVs.

time after rats were treated with NSS or DOXO, we found that on day 30, the average levels of 4HNE-adducted protein increased significantly in the DOXO-treated group compared to baseline and remained elevated at endpoint. In contrast, there was no change in 4HNE-adducted protein in the EVs of the NSS group. (Fig. 4**A**). Moreover, on day 9, the DOXO group's 4HNE-adducted protein level was significantly higher than that of the NSS group. Since the variation of 4HNE-adducted protein levels was quite high in the DOXO group, subgroup analysis was performed: those that survived until the endpoint (DOXO_Survive) and those that did not (DOXO_Not survive). We observed significantly lower levels of 4HNE-adducted protein in the DOXO_Not survive group (Fig. 4**B**). At day 30 post-treatment, the trend of reduced levels of 4HNE-adducted protein in the DOXO_Not survive group persisted (Fig. 4**C**).

4HNE-adducted protein levels in EVs were correlated with oxidative stress level, cardiac oxidative defense response, and cardiac function

We analyzed the relationship of 4HNE-adducted protein levels in serum EVs from each time point to the endpoint levels of 4HNE adduction in heart tissue, *Cat* and *Gpx1* gene expression, and cardiac functions including %LVEF and %LVFS. Correlations were found of the 4HNE-adducted protein levels in EVs at day 9 between the DOXO- and NSS-treated groups for: 4HNE-adducted protein levels (r = 0.6915), *Cat* gene expression levels (r = 0.7488), and *Gpx1* gene expression levels (r = 0.6083) in heart tissues (Fig. 5**A-5C**). These findings suggested that as early as the ninth day following the start of treatment, the level of 4HNE-adducted protein in serum EVs could predict the degree of oxidative stress and antioxidant defensive capacity in DOXO-damaged cardiac tissues. In addition, the levels of 4HNE-adducted proteins in serum EVs at endpoint were negatively correlated with %LVEF and %LVFS (Fig. 5**D, 5F**), highlighting the clinical relevance of this oxidative biomarker.

We also detected levels of 4HNE-adducted protein in the serum; the result is depicted in **Supplementary Figure 1**. On day 9, the serum concentration of 4HNE-adducted protein in the DOXO-treated group increased significantly. At 30 days and the endpoint, however, the levels returned to their baselines. In addition, correlations between serum 4HNE-adducted protein level on day 9 and 4HNE-adducted protein levels in cardiac tissues, *Cat* and *Gpx1* gene expression were analyzed. There is no correlation between the serum 4HNE-adducted protein level on day 9 and the cardiac parameters listed in Supplemental Table 1.

Discussion

There is a growing emphasis on the use of biomarkers to detect cardiotoxicity before it becomes irreversible, as long-term cardiomyopathy is becoming more recognized among cancer survivors. This study investigated the dynamic changes in the cardiac damage marker NT-proBNP in serum and the oxidative stress marker 4HNE-adducted protein in serum EVs induced by DOXO. In addition, the relationships between these markers and cardiac tissue oxidative stress and cardiac function were assessed in a rat model of DOXO-induced cardiotoxicity. The major findings of this study included: 1) the levels of 4HNE-adducted protein in serum EVs on day 9 of DOXO-treated rats began to differ from those in the NSS-treated rats, whereas NT-proBNP levels did not distinguish the two groups at the same timepoint; 2) rats that

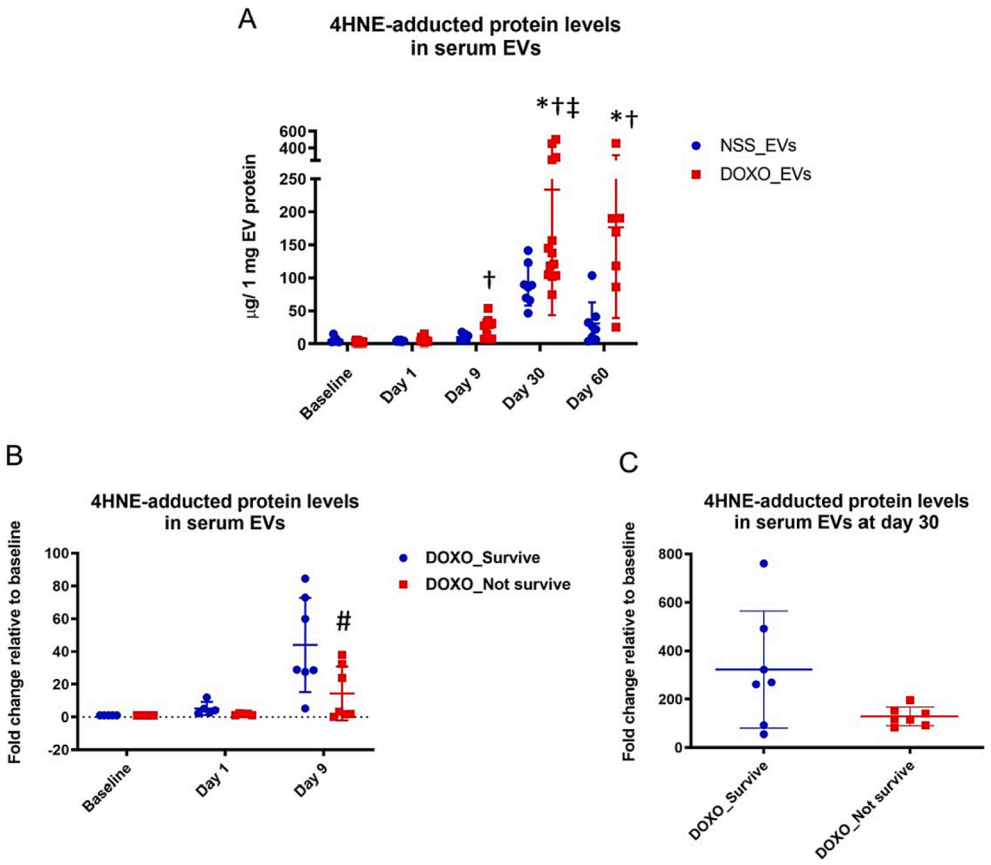

Fig. 4. Levels of 4HNE-adducted protein (μg/ 1 mg EV protein) in NSS_EVs and DOXO-EVs collected at each time point (A). Levels of 4HNE-adducted protein (fold change relative to baseline) at baseline, on day 1 and day 9 of DOXO-treated rats that survive until the endpoint (DOXO_Survive) and did not (DOXO_Not survive) (B). Levels of 4HNE-adducted protein (fold change relative to baseline) on day 30 comparing the DOXO_Survive and DOXO_Not survive groups (C). * $p < 0.05$ vs baseline, † $p < 0.05$ vs NSS_EVs at the same time point, ‡ $p < 0.05$ vs DOXO_EVs on day 9, # $p < 0.05$ vs DOXO_Survive.

endured DOXO toxicity until day 60 (the study endpoint) following treatment initiation contained a greater amount of 4HNE-adducted protein in serum EVs on day 9; 3) the level of 4HNE-adducted protein in serum EVs on day 9 was positively correlated with the level of 4HNE-adducted protein, *Cat*, and *Gpx1* gene expression in cardiac tissue; 4) cardiac function was negatively correlated with serum EV level of 4HNE-adducted protein at endpoint. According to these findings, the 4HNE-adducted protein in serum EVs might be used as an early non-invasive biological marker of an oxidative stress response to DOXO-induced cardiomyopathy.

Because DOXO-induced cardiomyopathy in cancer patients takes many years to develop following the initiation of treatment, laboratory animals are utilized to study the toxicity of DOXO. Due to the rapid development of DOXO-induced cardiomyopathy in rodents in comparison to humans, they are frequently utilized as animal models for studying pathophysiology and potential biomarkers. Despite the absence of a universally accepted model for chronic cardiotoxicity of DOXO in rats, commonly used long-term treatment models with DOXO 1–5 mg/kg once weekly for 2–12 weeks at a cumulative dose of 3–25 mg/kg are found suitable for evaluating chronic cardiotoxicity (Podyacheva et al., 2021). Our research team developed a rat model of chronic DOXO treatment at the dosage of 3 mg/kg every four days for three times, followed by once per week for three weeks, totaling 18 mg/kg, and discovered that 30 days after the last treatment (60 days after the treatment's initiation), the rats had impaired cardiac function (Arinno et al., 2021; Chunchai et al., 2022; Khuanjing et al., 2021; Maneechote et al., 2022; Yarana et al., 2022). Using the same treatment protocol, the current study demonstrated that the levels of NT-proBNP in the DOXO group were substantially higher than those in the NSS group at day 30 and 60 after beginning treatment, indicating the development of cardiotoxic effects. Intriguingly, NT-proBNP levels in the NSS group increased from baseline on day 9 and remained elevated until the end of the study. This result could be due to the fact that the anesthetic agent isoflurane has been shown to induce hypoxia inducible factor-1 alpha (HIF-1alpha) in a concentration- and time-dependent manner (Li et al., 2006), resulting in BNP mRNA upregulation since it is an HIF-1 alpha specific target gene (Weidemann et al., 2008).

Extracellular vesicles are small enclosed membranous particles discharged from cells into the extracellular milieu. Their intricate cargo reflects the (patho)physiological condition of the cells from which they originate. Such cargo is protected from enzymatic degradation and is therefore very stable in the extracellular environment. In addition, the presence of these EVs in peripheral body fluids permits minimally invasive liquid biopsies of biomolecules that reflect molecular events occurring in inaccessible organs, such as heart and brain. These characteristics explain the dramatic increase in interest in EVs during the past decade as carrying potential biomarkers or novel delivering treatments (Ciferri et al., 2021; Picca et al., 2022).

It has been hypothesized that small EVs, also known as exosomes, may contribute to the regulation and control of cellular homeostasis by facilitating the selective release of intracellular toxins, such as proteins, lipids, and nucleic acids (Baixauli et al., 2014; Desdin-Mico & Mittelbrunn, 2017). Multiple lines of evidence suggest that the analysis of EVs and their cargos can inform therapeutic strategy determinations for better-stratified cancer therapy (Irmer et al., 2023; Shi et al., 2020; Stevic et al., 2018; Zare et al., 2019; Zhou et al., 2021). Specifically, variations in EVs and their cargos before and after therapy can provide real-time information on therapeutic responses in cancer patients,

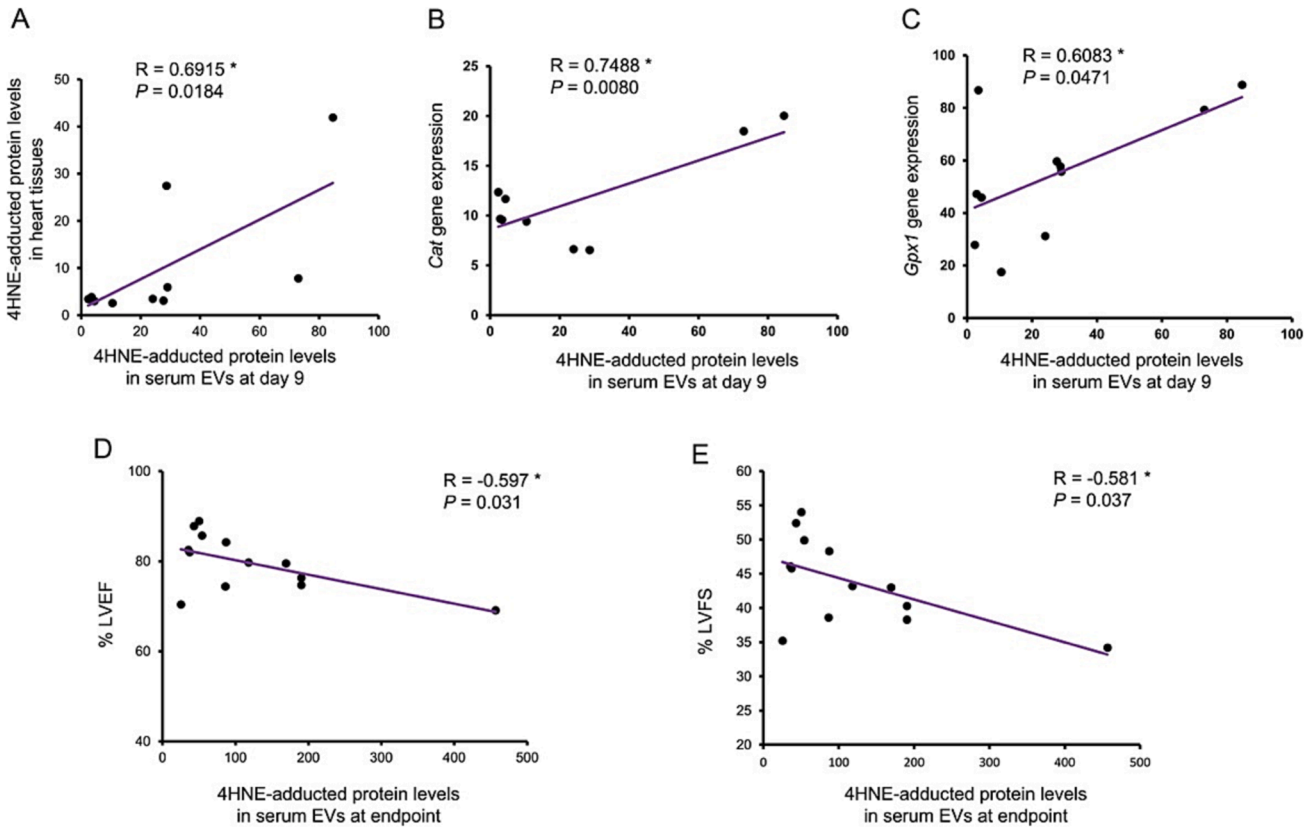

Fig. 5. Correlation graph of 4HNE-adducted protein levels in serum EVs at day 9 and 4HNE adducted protein levels in heart tissues (A). Correlation graph of 4HNE-adducted protein level in serum EVs at day 9 and *Cat* mRNA copy number relative to *Actb* in heart tissues (B). Correlation graph of 4HNE-adducted protein levels in serum EVs at day 9 and *Gpx1* mRNA copy number relative to *Actb* in heart tissues (C). Correlation graph of 4HNE-adducted protein level in serum EVs at the endpoint and left ventricular ejection fraction (%LVEF) at endpoint (D). Correlation graph of 4HNE-adducted protein level in serum EVs at endpoint and left ventricular fractional shortening (%LVFS) at endpoint (E). R = Pearson correlation coefficient, $P = p$ value, * $p < 0.05$.

including the common problem of therapy resistance. However, none of the clinical studies reveal a correlation between EVs and chemotherapy-related organ toxicity. The dynamic examination of circulating EVs and their constituents can facilitate hierarchical management and individualized cancer patient treatment. In this study, the size distribution data suggested that the isolated EVs were small EVs according to the Minimal Information for the Study of Extracellular Vesicles (MISEV) 2018 guideline (Thery et al., 2018). In addition, we found that the concentration of EVs in the NSS group increased substantially at day 30 post-treatment, exceeding that of the DOXO group. The reason might be due to the recurrent blood collection via tail veins that required inhalation of isoflurane for anesthesia. Although the mechanisms are unknown, it has been observed that anesthetic drugs may cause exosome release in rats (Piao et al., 2022), possibly by activating certain neurotransmitters and their associated ion channels throughout the body (Hemmings, 2009). Since these rats also experienced the same protocol as that in NSS group, the concentration of EVs should be high too in the DOXO group. However, the concentrations of serum EVs in DOXO groups only slightly elevated after DOXO treatment, when compared to the NSS group. This could be due to the fact that DOXO inhibits DNA synthesis and, as a result, suppresses hematopoiesis (Sonneveld et al., 1981), resulting in a decrease in the number of platelets, erythrocytes, and other blood cells, which are significant sources of circulating EVs (Thangaraju et al., 2020). Therefore, the concentration of EVs in the DOXO group was higher than in the NSS group at the endpoint since there was no bone marrow suppression effect at this period despite the ongoing oxidative stress, which could be the inducer of EV release.

Despite the small changes in concentration of the serum EVs in the DOXO group, there was a significant increase in 4HNE-adducted protein levels in serum EVs compared to those in the NSS-treated rats starting at day 9. Furthermore, among DOXO-treated rats, those with higher amounts of 4HNE-adducted protein in EVs on day 9 tolerated the toxicity better than those with lower level. These findings suggested that 4HNE-adducted proteins in serum EVs could be an early biomarker of resistance to DOXO-induced oxidative stress and can predict survival outcome. In addition, the alterations in 4HNE-adducted protein in EVs occurred before serum changes in NT-proBNP, the traditional cardiac marker. These results are consistent with a previous report in which oxidative homeostasis was found to be disturbed as early as 7 days after DOX treatment and that these changes happened before the significant rise in NT-proBNP (Dulf et al., 2023).

The lipid peroxidation byproduct known as 4HNE is one of the most bioactive and researched lipid aldehydes (Benedetti et al., 1980). Through the formation of covalent adducts with nucleophilic functional groups in proteins, nucleic acids, and membrane lipids, 4HNE can modify a variety of signaling processes linked to organ dysfunction due to oxidative stress (Zhong & Yin, 2015). 4HNE protein adducts have been found to be indicators of oxidative stress in several cardiovascular disorders (Mali & Palaniyandi, 2014), such as atherosclerosis (Selley et al., 1998), myocardial ischemia–reperfusion injury (Eaton et al., 1999), heart failure (Coirault et al., 2007), and cardiomyopathy (Asselin et al., 2007). There is a clinical investigation conducted on cancer patients who were administered DOXO as part of their treatment protocol, excluding any additional free-radical scavenging agents, revealed a significant increase in plasma levels of 4HNE (Aluise et al., 2011). In animal models, increased 4HNE adducted protein in cardiac mitochondria as a result of DOXO therapy results in mitochondrial dysfunction (Kavazis et al., 2010; Miriyala et al., 2016). In this study, a significant

increase in 4HNE adduction in heart tissues in the DOXO group was found at study endpoint. Although DOXO itself cannot cross the blood–brain barrier (BBB), prior studies using mice treated with a single 20 mg/kg dose of DOXO demonstrated that DOXO increased peripheral tumor necrosis factor (TNF-alpha), which could cross the BBB and caused oxidative stress, leading to cognitive decline known as "chemo-brain". (Joshi et al., 2010; Joshi et al., 2007; Joshi et al., 2005; Tangpong et al., 2006). Thus, we also measured 4HNE adduction and oxidative stress response in brain tissue. Since the level of 4HNE adduction did not change in brain tissue, where DOXO cannot enter, the rise in 4HNE adduction was specifically related to oxidative stress caused by DOXO in the heart.

4HNE has been identified as a growth-regulating factor that participates in redox signaling under both physiological and pathophysiological conditions. Redox signaling processes induced by 4HNE are complex and vary depending on the concentration of 4HNE, the molecules targeted, and the cell type (Jaganjac et al., 2020). For instance, low levels of 4HNE ($\leq$1 μM) provoke neovascularization via ROS and activation of sphingolipid pathway in endothelial cells (Camare et al., 2017). At concentrations 5–10 μM, 4HNE specifically targets and modifies proteins involved in the autophagy initiation. On the contrary, at higher concentration ($\geq$15 μM), 4HNE suppresses autophagy inducing mitochondrial dysfunction in primary neurons (Dodson et al., 2017). A study using mouse cardiomyocytes (Lopez-Bernardo et al., 2015) revealed that concentrations of 4HNE 5–20 μM can activate protective pathways, including the Nrf2 (nuclear factor erythroid 2-related factor 2), which is a transcription factor responsible for the upregulation of multiple antioxidant enzymes (such as thioredoxin, thioredoxin reductase, sulfiredoxin, peroxiredoxin, glutathione peroxidase, superoxide dismutase 1, catalase, and several glutathione S-transferases) (He et al., 2020). The minimally increased level of 4HNE adduction in serum EVs at day 9 of our study might indicate that a low level of intracellular oxidative stress occurred in heart tissues and thus explain the correlations with levels of 4HNE-adducted protein, and of *Cat* and *Gpx1* gene expression in heart tissues at endpoint. DOXO-treated rats with high levels of 4HNE adduction in serum EVs on day 9 might be survive to the endpoint due to a greater Nrf2 response since it is a crucial protective mechanism under oxidative stress conditions. Such correlations make 4HNE adduction in serum EVs a possible early (day 9) predictor of patients susceptible to DOXO-induced cardiotoxicity. In contrast to the levels at day 9, levels of 4HNE-adducted proteins in serum EVs at endpoint were correlated with poor cardiac functions including lower %LVEF and %LVFS. The explanation of these data may be due to the persistently elevated levels of oxidative stress which could lead to severe irreversible cardiac dysfunction. Since 4HNE have pleiotropic biological effect, an integrative biomedicine approach that is aware of the pathophysiological functions of 4HNE should be utilized to treat stress-related diseases such as doxorubicin-induced cardiotoxicity (Jaganjac et al., 2020).

The positive correlation of 4HNE adduction in serum EVs with *Cat* and *Gpx1* gene expression in heart tissues is consistent with our previous *in vitro* study finding, which demonstrated that EVs extracted from serum of DOXO-treated animals at the endpoint effectively reduced ROS formation of H9c2 cardiomyocytes via increased *Cat* and *Gpx1* gene expression and reduced hydrogen peroxide-induced cell death (Yarana et al., 2022). Further animal studies should be conducted to increase the protective impact of EVs on cardiac function by pretreating animals with DOXO_EVs prior to DOXO administration and determining whether these EV-treated rats had improved cardiac functions compared to those who did not get EV pretreatment.

Conclusion

This study demonstrated that DOXO-treated rats with low levels of 4HNE-adducted proteins in serum EVs at day 9 were more susceptible to toxicity and poor survival outcomes. These levels were positively correlated with indicators of oxidative stress and antioxidant defense capacity of the heart tissues. In contrast, 4HNE-adducted protein levels in serum EVs 30 days after end of treatment were negatively correlated with impaired cardiac functions. Our findings indicate that the level of 4HNE-adducted protein in serum EVs may serve as an early, minimally invasive biomarker reflecting the risk of DOXO-induced cardiomyopathy. Monitoring the cardiotoxicity risk as early as feasible is essential for adjusting the chemotherapy regimen and applying cardioprotective intervention in an individualized manner to prevent the onset and progression of chemotherapy-induced cardiotoxicity. Additional research on the correlation between 4HNE-adducted protein levels in serum EVs of cancer patients who received DOXO and long-term cardiomyopathy outcome should be done to confirm this speculation.

Declaration of generative AI and AI- assisted technologies in the writing process

During the preparation of this work the authors used QuillBot in order to paraphrase sentences to make them more comprehensible and to check English grammar. After using this tool/service and consulting with a native speaker, the authors reviewed and edited the content as needed and take full responsibility for the content of the publication.

CRediT authorship contribution statement

Chontida Yarana: Conceptualization, Data curation, Formal analysis, Funding acquisition, Investigation, Methodology, Project administration, Writing – original draft. **Chayodom Maneechote:** Data curation, Formal analysis, Investigation, Methodology. **Thawatchai Khuanjing:** Data curation, Formal analysis, Investigation, Methodology. **Benjamin Ongnok:** Data curation, Formal analysis, Investigation, Methodology. **Nanthip Prathumsap:** Data curation, Formal analysis, Investigation, Methodology. **Sirasa Thanasrisuk:** Data curation, Formal analysis. **Kovit Pattanapanyasat:** Supervision, Writing – review & editing. **Siriporn C. Chattipakorn:** Resources, Supervision, Funding acquisition, Writing – review & editing. **Nipon Chattipakorn:** Conceptualization, Resources, Supervision, Funding acquisition, Writing – review & editing.

Declaration of Competing Interest

The authors declare that they have no known competing financial interests or personal relationships that could have appeared to influence the work reported in this paper.

Data availability

Data will be made available on request.

Acknowledgements

This work (Grant No. RGNS63-162) was financially supported by Office of the Permanent Secretary, Ministry of Higher Education, Science, Research and Innovation (OPS MHESI), Thailand Science Research and Innovation (TSRI) (to C.Y.). High-Potential Research Team Grant Program, grant number N42A650870 (to K.P.). Center of Excellence Award from Chiang Mai University (to N.C.).

Appendix A. Supplementary data

Supplementary data to this article can be found online at https://doi.org/10.1016/j.crtox.2023.100134.

References

Aluise, C.D., Miriyala, S., Noel, T., Sultana, R., Jungsuwadee, P., Taylor, T.J., Cai, J., Pierce, W.M., Vore, M., Moscow, J.A., St Clair, D.K., Butterfield, D.A., 2011. 2-Mercaptoethane sulfonate prevents doxorubicin-induced plasma protein oxidation and TNF-alpha release: implications for the reactive oxygen species-mediated mechanisms of chemobrain. Free Radic. Biol. Med. 50 (11), 1630–1638. https://doi.org/10.1016/j.freeradbiomed.2011.03.009.

Arinno, A., Maneechote, C., Khuanjing, T., Ongnok, B., Prathumsap, N., Chunchai, T., Arunsak, B., Kerdphoo, S., Shinlapawittayatorn, K., Chattipakorn, S.C., Chattipakorn, N., 2021. Cardioprotective effects of melatonin and metformin against doxorubicin-induced cardiotoxicity in rats are through preserving mitochondrial function and dynamics. Biochem. Pharmacol. 192, 114743 https://doi.org/10.1016/j.bcp.2021.114743.

Asselin, C., Shi, Y., Clement, R., Tardif, J.C., Des Rosiers, C., 2007. Higher circulating 4-hydroxynonenal-protein thioether adducts correlate with more severe diastolic dysfunction in spontaneously hypertensive rats. Redox Rep. 12 (1), 68–72. https://doi.org/10.1179/135100007X162202.

Baixauli, F., Lopez-Otin, C., Mittelbrunn, M., 2014. Exosomes and autophagy: coordinated mechanisms for the maintenance of cellular fitness. Front. Immunol. 5, 403. https://doi.org/10.3389/fimmu.2014.00403.

Benedetti, A., Comporti, M., Esterbauer, H., 1980. Identification of 4-hydroxynonenal as a cytotoxic product originating from the peroxidation of liver microsomal lipids. BBA 620 (2), 281–296. https://doi.org/10.1016/0005-2760(80)90209-x.

Benedikter, B.J., Weseler, A.R., Wouters, E.F.M., Savelkoul, P.H.M., Rohde, G.G.U., Stassen, F.R.M., 2018. Redox-dependent thiol modifications: implications for the release of extracellular vesicles. Cell. Mol. Life Sci. 75 (13), 2321–2337. https://doi.org/10.1007/s00018-018-2806-z.

Billinge, E.R., Broom, M., Platt, M., 2014. Monitoring aptamer-protein interactions using tunable resistive pulse sensing. Anal. Chem. 86 (2), 1030–1037. https://doi.org/10.1021/ac401764c.

Camare, C., Vanucci-Bacque, C., Auge, N., Pucelle, M., Bernis, C., Swiader, A., Baltas, M., Bedos-Belval, F., Salvayre, R., Negre-Salvayre, A., 2017. 4-hydroxynonenal contributes to angiogenesis through a redox-dependent sphingolipid pathway: prevention by hydralazine derivatives. Oxid. Med. Cell. Longev. 2017, 9172741. https://doi.org/10.1155/2017/9172741.

Campanella, C., Caruso Bavisotto, C., Logozzi, M., Marino Gammazza, A., Mizzoni, D., Cappello, F., Fais, S., 2019. On the choice of the extracellular vesicles for therapeutic purposes. Int. J. Mol. Sci. 20 (2) https://doi.org/10.3390/ijms20020236.

Chaiswing, L., Cole, M.P., Ittarat, W., Szweda, L.I., St Clair, D.K., Oberley, T.D., 2005. Manganese superoxide dismutase and inducible nitric oxide synthase modify early oxidative events in acute adriamycin-induced mitochondrial toxicity. Mol. Cancer Ther. 4 (7), 1056–1064. https://doi.org/10.1158/1535-7163.MCT-04-0322.

Chapple, S.J., Cheng, X., Mann, G.E., 2013. Effects of 4-hydroxynonenal on vascular endothelial and smooth muscle cell redox signaling and function in health and disease. Redox Biol. 1 (1), 319–331. https://doi.org/10.1016/j.redox.2013.04.001.

Cheng, J., Wang, X., Yuan, X., Liu, G., Chu, Q., 2022. Emerging roles of exosome-derived biomarkers in cancer theranostics: messages from novel protein targets. Am. J. Cancer Res. 12 (5), 2226–2248. https://www.ncbi.nlm.nih.gov/pubmed/35693088.

Chiaradia, E., Tancini, B., Emiliani, C., Delo, F., Pellegrino, R.M., Tognoloni, A., Urbanelli, L., Buratta, S., 2021. Extracellular vesicles under oxidative stress conditions biological properties and physiological roles. Cells 10 (7). https://doi.org/10.3390/cells10071763.

Chow, S. L., Maisel, A. S., Anand, I., Bozkurt, B., de Boer, R. A., Felker, G. M., Fonarow, G. C., Greenberg, B., Januzzi, J. L., Jr., Kiernan, M. S., Liu, P. P., Wang, T. J., Yancy, C. W., Zile, M. R., American Heart Association Clinical Pharmacology Committee of the Council on Clinical, C., Council on Basic Cardiovascular, S., Council on Cardiovascular Disease in the, Y., Council on, C., Stroke, N., . . . Outcomes, R. (2017). Role of biomarkers for the prevention, assessment, and management of heart failure: a scientific statement from the american heart association. Circulation, 135(22), e1054-e1091. https://doi.org/10.1161/CIR.0000000000000490.

Chunchai, T., Arinno, A., Ongnok, B., Pantiya, P., Khuanjing, T., Prathumsap, N., Maneechote, C., Chattipakorn, N., Chattipakorn, S.C., 2022. Ranolazine alleviated cardiac/brain dysfunction in doxorubicin-treated rats. Exp. Mol. Pathol. 127, 104818 https://doi.org/10.1016/j.yexmp.2022.104818.

Ciferri, M.C., Quarto, R., Tasso, R., 2021. Extracellular vesicles as biomarkers and therapeutic tools: from pre-clinical to clinical applications. Biology (basel) 10 (5). https://doi.org/10.3390/biology10050359.

Coirault, C., Guellich, A., Barbry, T., Samuel, J.L., Riou, B., Lecarpentier, Y., 2007. Oxidative stress of myosin contributes to skeletal muscle dysfunction in rats with chronic heart failure. Am. J. Phys. Heart Circ. Phys. 292 (2), H1009–H1017. https://doi.org/10.1152/ajpheart.00438.2006.

Desdin-Mico, G., Mittelbrunn, M., 2017. Role of exosomes in the protection of cellular homeostasis. Cell Adh. Migr. 11 (2), 127–134. https://doi.org/10.1080/19336918.2016.1251000.

Dodson, M., Wani, W.Y., Redmann, M., Benavides, G.A., Johnson, M.S., Ouyang, X., Cofield, S.S., Mitra, K., Darley-Usmar, V., Zhang, J., 2017. Regulation of autophagy, mitochondrial dynamics, and cellular bioenergetics by 4-hydroxynonenal in primary neurons. Autophagy 13 (11), 1828–1840. https://doi.org/10.1080/15548627.2017.1356948.

Dulf, P.L., Mocan, M., Coada, C.A., Dulf, D.V., Moldovan, R., Baldea, I., Farcas, A.D., Blendea, D., Filip, A.G., 2023. Doxorubicin-induced acute cardiotoxicity is associated with increased oxidative stress, autophagy, and inflammation in a murine model. Naunyn Schmiedebergs Arch. Pharmacol. 396 (6), 1105–1115. https://doi.org/10.1007/s00210-023-02382-z.

Eaton, P., Li, J.M., Hearse, D.J., Shattock, M.J., 1999. Formation of 4-hydroxy-2-nonenal-modified proteins in ischemic rat heart. Am. J. Phys. Anthropol. 276 (3), H935–H943. https://doi.org/10.1152/ajpheart.1999.276.3.H935.

Gao, R., Lv, C., Qu, Y., Yang, H., Hao, C., Sun, X., Hu, X., Yang, Y., Tang, Y., 2023. Remote ischemic conditioning mediates cardio-protection after myocardial ischemia/reperfusion injury by reducing 4-hne levels and regulating autophagy via the ALDH2/SIRT3/HIF1alpha signaling pathway. J. Cardiovasc. Transl. Res. https://doi.org/10.1007/s12265-023-10355-z.

Hammarsten, O., Wernbom, M., Mills, N.L., Mueller, C., 2022. How is cardiac troponin released from cardiomyocytes? Eur. Heart J. Acute Cardiovasc. Care 11 (9), 718–720. https://doi.org/10.1093/ehjacc/zuac091.

He, F., Ru, X., Wen, T., 2020. NRF2, a transcription factor for stress response and beyond. Int. J. Mol. Sci. 21 (13) https://doi.org/10.3390/ijms21134777.

Hemmings Jr., H.C., 2009. Sodium channels and the synaptic mechanisms of inhaled anaesthetics. Br. J. Anaesth. 103 (1), 61–69. https://doi.org/10.1093/bja/aep144.

Hwang, H.V., Sandeep, N., Paige, S.L., Ranjbarvaziri, S., Hu, D.Q., Zhao, M., Lan, I.S., Coronado, M., Kooiker, K.B., Wu, S.M., Fajardo, G., Bernstein, D., Reddy, S., 2020. 4HNE impairs myocardial bioenergetics in congenital heart disease-induced right ventricular failure. Circulation 142 (17), 1667–1683. https://doi.org/10.1161/CIRCULATIONAHA.120.045470.

Ibanez, B., James, S., Agewall, S., Antunes, M. J., Bucciarelli-Ducci, C., Bueno, H., Caforio, A. L. P., Crea, F., Goudevenos, J. A., Halvorsen, S., Hindricks, G., Kastrati, A., Lenzen, M. J., Prescott, E., Roffi, M., Valgimigli, M., Varenhorst, C., Vranckx, P., Widimsky, P., & Group, E. S. C. S. D. (2018). 2017 ESC Guidelines for the management of acute myocardial infarction in patients presenting with ST-segment elevation: The Task Force for the management of acute myocardial infarction in patients presenting with ST-segment elevation of the European Society of Cardiology (ESC). Eur Heart J, 39(2), 119-177. https://doi.org/10.1093/eurheartj/ehx393.

Irmer, B., Chandrabalan, S., Maas, L., Bleckmann, A., Menck, K., 2023. Extracellular vesicles in liquid biopsies as biomarkers for solid tumors. Cancers (basel) 15 (4). https://doi.org/10.3390/cancers15041307.

Jaganjac, M., Milkovic, L., Gegotek, A., Cindric, M., Zarkovic, K., Skrzydlewska, E., Zarkovic, N., 2020. The relevance of pathophysiological alterations in redox signaling of 4-hydroxynonenal for pharmacological therapies of major stress-associated diseases. Free Radic. Biol. Med. 157, 128–153. https://doi.org/10.1016/j.freeradbiomed.2019.11.023.

Joshi, G., Sultana, R., Tangpong, J., Cole, M.P., St Clair, D.K., Vore, M., Estus, S., Butterfield, D.A., 2005. Free radical mediated oxidative stress and toxic side effects in brain induced by the anti cancer drug adriamycin: insight into chemobrain. Free Radic. Res. 39 (11), 1147–1154. https://doi.org/10.1080/10715760500143478.

Joshi, G., Hardas, S., Sultana, R., St Clair, D.K., Vore, M., Butterfield, D.A., 2007. Glutathione elevation by gamma-glutamyl cysteine ethyl ester as a potential therapeutic strategy for preventing oxidative stress in brain mediated by in vivo administration of adriamycin: Implication for chemobrain. J. Neurosci. Res. 85 (3), 497–503. https://doi.org/10.1002/jnr.21158.

Joshi, G., Aluise, C.D., Cole, M.P., Sultana, R., Pierce, W.M., Vore, M., St Clair, D.K., Butterfield, D.A., 2010. Alterations in brain antioxidant enzymes and redox proteomic identification of oxidized brain proteins induced by the anti-cancer drug adriamycin: implications for oxidative stress-mediated chemobrain. Neuroscience 166 (3), 796–807. https://doi.org/10.1016/j.neuroscience.2010.01.021.

Jungsuwadee, P., Cole, M.P., Sultana, R., Joshi, G., Tangpong, J., Butterfield, D.A., St Clair, D.K., Vore, M., 2006. Increase in Mrp1 expression and 4-hydroxy-2-nonenal adduction in heart tissue of Adriamycin-treated C57BL/6 mice. Mol. Cancer Ther. 5 (11), 2851–2860. https://doi.org/10.1158/1535-7163.MCT-06-0297.

Jungsuwadee, P., Nithipongvanitch, R., Chen, Y., Oberley, T.D., Butterfield, D.A., St Clair, D.K., Vore, M., 2009. Mrp1 localization and function in cardiac mitochondria after doxorubicin. Mol. Pharmacol. 75 (5), 1117–1126. https://doi.org/10.1124/mol.108.052209.

Kavazis, A.N., Smuder, A.J., Min, K., Tumer, N., Powers, S.K., 2010. Short-term exercise training protects against doxorubicin-induced cardiac mitochondrial damage independent of HSP72. Am. J. Phys. Heart Circ. Phys. 299 (5), H1515–H1524. https://doi.org/10.1152/ajpheart.00585.2010.

Khuanjing, T., Ongnok, B., Maneechote, C., Siri-Angkul, N., Prathumsap, N., Arinno, A., Chunchai, T., Arunsak, B., Chattipakorn, S.C., Chattipakorn, N., 2021. Acetylcholinesterase inhibitor ameliorates doxorubicin-induced cardiotoxicity through reducing RIP1-mediated necroptosis. Pharmacol. Res. 173, 105882 https://doi.org/10.1016/j.phrs.2021.105882.

Kittiwarawut, A., Vorasettakarnkij, Y., Tanasanvimon, S., Manasnayakorn, S., Sriuranpong, V., 2013. Serum NT-proBNP in the early detection of doxorubicin-induced cardiac dysfunction. Asia Pac. J. Clin. Oncol. 9 (2), 155–161. https://doi.org/10.1111/j.1743-7563.2012.01588.x.

Leonarduzzi, G., Chiarpotto, E., Biasi, F., Poli, G., 2005. 4-Hydroxynonenal and cholesterol oxidation products in atherosclerosis. Mol. Nutr. Food Res. 49 (11), 1044–1049. https://doi.org/10.1002/mnfr.200500090.

Li, Q.F., Wang, X.R., Yang, Y.W., Su, D.S., 2006. Up-regulation of hypoxia inducible factor 1alpha by isoflurane in Hep3B cells. Anesthesiology 105 (6), 1211–1219. https://doi.org/10.1097/00000542-200612000-00021.

Lopez-Bernardo, E., Anedda, A., Sanchez-Perez, P., Acosta-Iborra, B., Cadenas, S., 2015. 4-Hydroxynonenal induces Nrf2-mediated UCP3 upregulation in mouse cardiomyocytes. Free Radic. Biol. Med. 88 (Pt B), 427–438. https://doi.org/10.1016/j.freeradbiomed.2015.03.032.

Maalouf, R., Bailey, S., 2016. A review on B-type natriuretic peptide monitoring: assays and biosensors. Heart Fail. Rev. 21 (5), 567–578. https://doi.org/10.1007/s10741-016-9544-9.

Mali, V.R., Palaniyandi, S.S., 2014. Regulation and therapeutic strategies of 4-hydroxy-2-nonenal metabolism in heart disease. Free Radic. Res. 48 (3), 251–263. https://doi.org/10.3109/10715762.2013.864761.

Maneechote, C., Palee, S., Apaijai, N., Kerdphoo, S., Jaiwongkam, T., Chattipakorn, S.C., Chattipakorn, N., 2019. Mitochondrial dynamic modulation exerts cardiometabolic protection in obese insulin-resistant rats. Clin. Sci. (Lond.) 133 (24), 2431–2447. https://doi.org/10.1042/CS20190960.

Maneechote, C., Khuanjing, T., Ongnok, B., Arinno, A., Prathumsap, N., Chunchai, T., Arunsak, B., Nawara, W., Chattipakorn, S.C., Chattipakorn, N., 2022. Promoting mitochondrial fusion in doxorubicin-induced cardiotoxicity: a novel therapeutic target for cardioprotection. Clin. Sci. (Lond.) 136 (11), 841–860. https://doi.org/10.1042/CS20220074.

Miriyala, S., Thippakorn, C., Chaiswing, L., Xu, Y., Noel, T., Tovmasyan, A., Batinic-Haberle, I., Vander Kooi, C.W., Chi, W., Latif, A.A., Panchatcharam, M., Prachayasittikul, V., Butterfield, D.A., Vore, M., Moscow, J., St Clair, D.K., 2016. Novel role of 4-hydroxy-2-nonenal in AIFm2-mediated mitochondrial stress signaling. Free Radic. Biol. Med. 91, 68–80. https://doi.org/10.1016/j.freeradbiomed.2015.12.002.

Negre-Salvayre, A., Auge, N., Ayala, V., Basaga, H., Boada, J., Brenke, R., Chapple, S., Cohen, G., Feher, J., Grune, T., Lengyel, G., Mann, G.E., Pamplona, R., Poli, G., Portero-Otin, M., Riahi, Y., Salvayre, R., Sasson, S., Serrano, J., Zarkovic, N., 2010. Pathological aspects of lipid peroxidation. Free Radic. Res. 44 (10), 1125–1171. https://doi.org/10.3109/10715762.2010.498478.

Newby, L.K., Rodriguez, I., Finkle, J., Becker, R.C., Hicks, K.A., Hausner, E., Chesler, R., Harper, C., Targum, S., Berridge, B.R., Lewis, E., Walker, D.B., Dollery, C., Turner, J. R., Krucoff, M.W., 2011. Troponin measurements during drug development–considerations for monitoring and management of potential cardiotoxicity: an educational collaboration among the Cardiac Safety Research Consortium, the Duke Clinical Research Institute, and the US Food and Drug Administration. Am. Heart J. 162 (1), 64–73. https://doi.org/10.1016/j.ahj.2011.04.005.

Nizamudeen, Z., Markus, R., Lodge, R., Parmenter, C., Platt, M., Chakrabarti, L., Sottile, V., 2018. Rapid and accurate analysis of stem cell-derived extracellular vesicles with super resolution microscopy and live imaging. Biochim. Biophys. Acta 1865 (12), 1891–1900. https://doi.org/10.1016/j.bbamcr.2018.09.008.

Piao, L., Na, O.H., Seo, E.H., Hong, S.W., Sohn, K.M., Kwon, Y., Lee, S.H., Kim, S.H., 2022. Effects of general anaesthesia with an inhalational anaesthetic agent on the expression of exosomes in rats. Int. J. Med. Sci. 19 (9), 1399–1407. https://doi.org/10.7150/ijms.72565.

Picca, A., Guerra, F., Calvani, R., Coelho-Junior, H.J., Bucci, C., Marzetti, E., 2022. Circulating extracellular vesicles: friends and foes in neurodegeneration. Neural Regen. Res. 17 (3), 534–542. https://doi.org/10.4103/1673-5374.320972.

Podyacheva, E.Y., Kushnareva, E.A., Karpov, A.A., Toropova, Y.G., 2021. Analysis of models of doxorubicin-induced cardiomyopathy in rats and mice. A modern view from the perspective of the pathophysiologist and the clinician. Front. Pharmacol. 12, 670479 https://doi.org/10.3389/fphar.2021.670479.

Sangweni, N.F., Gabuza, K., Huisamen, B., Mabasa, L., van Vuuren, D., Johnson, R., 2022. Molecular insights into the pathophysiology of doxorubicin-induced cardiotoxicity: a graphical representation. Arch. Toxicol. 96 (6), 1541–1550. https://doi.org/10.1007/s00204-022-03262-w.

Selley, M.L., Bartlett, M.R., Czeti, A.L., Ardlie, N.G., 1998. The role of (E)-4-hydroxy-2-nonenal in platelet activation by low density lipoprotein and iron. Atherosclerosis 140 (1), 105–112. https://doi.org/10.1016/s0021-9150(98)00123-3.

Shakir, D.K., Rasul, K.I., 2009. Chemotherapy induced cardiomyopathy: pathogenesis, monitoring and management. J. Clin. Med. Res. 1 (1), 8–12. https://doi.org/10.4021/jocmr2009.02.1225.

Sherief, L.M., Kamal, A.G., Khalek, E.A., Kamal, N.M., Soliman, A.A., Esh, A.M., 2012. Biomarkers and early detection of late onset anthracycline-induced cardiotoxicity in children. Hematology 17 (3), 151–156. https://doi.org/10.1179/102453312X13376952196412.

Shi, A., Kasumova, G.G., Michaud, W.A., Cintolo-Gonzalez, J., Diaz-Martinez, M., Ohmura, J., Mehta, A., Chien, I., Frederick, D.T., Cohen, S., Plana, D., Johnson, D., Flaherty, K.T., Sullivan, R.J., Kellis, M., Boland, G.M., 2020. Plasma-derived extracellular vesicle analysis and deconvolution enable prediction and tracking of melanoma checkpoint blockade outcome. Sci. Adv. 6 (46) https://doi.org/10.1126/sciadv.abb3461.

Singh, P., Sharma, R., McElhanon, K., Allen, C.D., Megyesi, J.K., Benes, H., Singh, S.P., 2015. Sulforaphane protects the heart from doxorubicin-induced toxicity. Free Radic. Biol. Med. 86, 90–101. https://doi.org/10.1016/j.freeradbiomed.2015.05.028.

Songbo, M., Lang, H., Xinyong, C., Bin, X., Ping, Z., Liang, S., 2019. Oxidative stress injury in doxorubicin-induced cardiotoxicity. Toxicol. Lett. 307, 41–48. https://doi.org/10.1016/j.toxlet.2019.02.013.

Sonneveld, P., Mulder, J., van Bekkum, D.W., 1981. Cytotoxicity of doxorubicin for normal hematopoietic and acute myeloid leukemia cells of the rat. Cancer Chemother. Pharmacol. 5 (3), 167–173. https://doi.org/10.1007/BF00258475.

Sorodoc, V., Sirbu, O., Lionte, C., Haliga, R.E., Stoica, A., Ceasovschih, A., Petris, O.R., Constantin, M., Costache, I.I., Petris, A.O., Morariu, P.C., Sorodoc, L., 2022. The value of troponin as a biomarker of chemotherapy-induced cardiotoxicity. Life (basel) 12 (8). https://doi.org/10.3390/life12081183.

Stevic, I., Muller, V., Weber, K., Fasching, P.A., Karn, T., Marme, F., Schem, C., Stickeler, E., Denkert, C., van Mackelenbergh, M., Salat, C., Schneeweiss, A., Pantel, K., Loibl, S., Untch, M., Schwarzenbach, H., 2018. Specific microRNA signatures in exosomes of triple-negative and HER2-positive breast cancer patients undergoing neoadjuvant therapy within the GeparSixto trial. BMC Med. 16 (1), 179. https://doi.org/10.1186/s12916-018-1163-y.

Sturgeon, K.M., Deng, L., Bluethmann, S.M., Zhou, S., Trifiletti, D.M., Jiang, C., Kelly, S. P., Zaorsky, N.G., 2019. A population-based study of cardiovascular disease mortality risk in US cancer patients. Eur. Heart J. 40 (48), 3889–3897. https://doi.org/10.1093/eurheartj/ehz766.

Sulaiman, L., Hesham, D., Abdel Hamid, M., Youssef, G., 2021. The combined role of NT-proBNP and LV-GLS in the detection of early subtle chemotherapy-induced cardiotoxicity in breast cancer female patients. Egypt Heart J 73 (1), 20. https://doi.org/10.1186/s43044-021-00142-z.

Tangpong, J., Cole, M.P., Sultana, R., Joshi, G., Estus, S., Vore, M., St Clair, W., Ratanachaiyavong, S., St Clair, D.K., Butterfield, D.A., 2006. Adriamycin-induced, TNF-alpha-mediated central nervous system toxicity. Neurobiol. Dis. 23 (1), 127–139. https://doi.org/10.1016/j.nbd.2006.02.013.

Thangaraju, K., Neerukonda, S.N., Katneni, U., Buehler, P.W., 2020. Extracellular vesicles from red blood cells and their evolving roles in health, coagulopathy and therapy. Int. J. Mol. Sci. 22 (1) https://doi.org/10.3390/ijms22010153.

Thery, C., Witwer, K.W., Aikawa, E., Alcaraz, M.J., Anderson, J.D., Andriantsitohaina, R., Antoniou, A., Arab, T., Archer, F., Atkin-Smith, G.K., Ayre, D.C., Bach, J.M., Bachurski, D., Baharvand, H., Balaj, L., Baldacchino, S., Bauer, N.N., Baxter, A.A., Bebawy, M., Zuba-Surma, E.K., 2018. Minimal information for studies of extracellular vesicles 2018 (MISEV2018): a position statement of the International Society for Extracellular Vesicles and update of the MISEV2014 guidelines. J. Extracell Vesicles 7 (1), 1535750. https://doi.org/10.1080/20013078.2018.1535750.

Tian, S., Hirshfield, K.M., Jabbour, S.K., Toppmeyer, D., Haffty, B.G., Khan, A.J., Goyal, S., 2014. Serum biomarkers for the detection of cardiac toxicity after chemotherapy and radiation therapy in breast cancer patients. Front. Oncol. 4, 277. https://doi.org/10.3389/fonc.2014.00277.

Troughton, R., Michael Felker, G., Januzzi Jr., J.L., 2014. Natriuretic peptide-guided heart failure management. Eur. Heart J. 35 (1), 16–24. https://doi.org/10.1093/eurheartj/eht463.

Vogel, R., Coumans, F.A., Maltesen, R.G., Boing, A.N., Bonnington, K.E., Broekman, M.L., Broom, M.F., Buzas, E.I., Christiansen, G., Hajji, N., Kristensen, S.R., Kuehn, M.J., Lund, S.M., Maas, S.L., Nieuwland, R., Osteikoetxea, X., Schnoor, R., Scicluna, B.J., Shambrook, M., Pedersen, S., 2016. A standardized method to determine the concentration of extracellular vesicles using tunable resistive pulse sensing. J. Extracell Vesicles 5, 31242. https://doi.org/10.3402/jev.v5.31242.

Watson, C., Gadikota, H., Barlev, A., Beckerman, R., 2022. A review of the risks of long-term consequences associated with components of the CHOP chemotherapy regimen. J Drug Assess 11 (1), 1–11. https://doi.org/10.1080/21556660.2022.2073101.

Weidemann, A., Klanke, B., Wagner, M., Volk, T., Willam, C., Wiesener, M.S., Eckardt, K. U., Warnecke, C., 2008. Hypoxia, via stabilization of the hypoxia-inducible factor HIF-1alpha, is a direct and sufficient stimulus for brain-type natriuretic peptide induction. Biochem. J 409 (1), 233–242. https://doi.org/10.1042/BJ20070629.

Yarana, C., Carroll, D., Chen, J., Chaiswing, L., Zhao, Y., Noel, T., Alstott, M., Bae, Y., Dressler, E.V., Moscow, J.A., Butterfield, D.A., Zhu, H., St Clair, D.K., 2018. Extracellular vesicles released by cardiomyocytes in a doxorubicin-induced cardiac injury mouse model contain protein biomarkers of early cardiac injury. Clin. Cancer Res. 24 (7), 1644–1653. https://doi.org/10.1158/1078-0432.CCR-17-2046.

Yarana, C., Siwaponanan, P., Maneechote, C., Khuanjing, T., Ongnok, B., Prathumsap, N., Chattipakorn, S.C., Chattipakorn, N., Pattanapanyasat, K., 2022. Extracellular vesicles released after doxorubicin treatment in rats protect cardiomyocytes from oxidative damage and induce pro-inflammatory gene expression in macrophages. Int. J. Mol. Sci. 23 (21) https://doi.org/10.3390/ijms232113465.

Yarana, C., St Clair, D.K., 2017. Chemotherapy-induced tissue injury: an insight into the role of extracellular vesicles-mediated oxidative stress responses. Antioxidants (basel) 6 (4). https://doi.org/10.3390/antiox6040075.

Yu, D., Li, Y., Wang, M., Gu, J., Xu, W., Cai, H., Fang, X., Zhang, X., 2022. Exosomes as a new frontier of cancer liquid biopsy. Mol. Cancer 21 (1), 56. https://doi.org/10.1186/s12943-022-01509-9.

Zare, N., Haghjooy Javanmard, S., Mehrzad, V., Eskandari, N., Kefayat, A., 2019. Evaluation of exosomal miR-155, let-7g and let-7i levels as a potential noninvasive biomarker among refractory/relapsed patients, responsive patients and patients receiving R-CHOP. Leuk. Lymphoma 60 (8), 1877–1889. https://doi.org/10.1080/10428194.2018.1563692.

Zhang, Y., Sano, M., Shinmura, K., Tamaki, K., Katsumata, Y., Matsuhashi, T., Morizane, S., Ito, H., Hishiki, T., Endo, J., Zhou, H., Yuasa, S., Kaneda, R., Suematsu, M., Fukuda, K., 2010. 4-hydroxy-2-nonenal protects against cardiac ischemia-reperfusion injury via the Nrf2-dependent pathway. J. Mol. Cell. Cardiol. 49 (4), 576–586. https://doi.org/10.1016/j.yjmcc.2010.05.011.

Zhong, H., Yin, H., 2015. Role of lipid peroxidation derived 4-hydroxynonenal (4-HNE) in cancer: focusing on mitochondria. Redox Biol. 4, 193–199. https://doi.org/10.1016/j.redox.2014.12.011.

Zhou, E., Li, Y., Wu, F., Guo, M., Xu, J., Wang, S., Tan, Q., Ma, P., Song, S., Jin, Y., 2021. Circulating extracellular vesicles are effective biomarkers for predicting response to cancer therapy. EBioMedicine 67, 103365. https://doi.org/10.1016/j.ebiom.2021.103365.

Zhou, B., Xu, K., Zheng, X., Chen, T., Wang, J., Song, Y., Shao, Y., Zheng, S., 2020. Application of exosomes as liquid biopsy in clinical diagnosis. Signal Transduct. Target. Ther. 5 (1), 144. https://doi.org/10.1038/s41392-020-00258-9.

Zidan, A., Sherief, L.M., El-sheikh, A., Saleh, S.H., Shahbah, D.A., Kamal, N.M., Sherbiny, H.S., Ahmad, H., 2015. NT-proBNP as early marker of subclinical late cardiotoxicity after doxorubicin therapy and mediastinal irradiation in childhood cancer survivors. Dis. Markers 2015, 513219. https://doi.org/10.1155/2015/513219.